

Charged-particle rapidity density in Au+Au collisions in a quark combination model

Feng-lan Shao,¹ Tao Yao,² and Qu-bing Xie²

¹*Department of Physics, Qufu Normal University, Shandong 273165, People's Republic of China*

²*Department of Physics, Shandong University, Shandong 250100, People's Republic of China*

Rapidity/seudorapidity densities for charged particles and their centrality, rapidity and energy dependence in Au+Au collisions at RHIC are studied in a quark combination model. Using a Gaussian-type rapidity distribution for constituent quarks as a result of Landau hydrodynamic evolution, the data at $\sqrt{s_{NN}} = 130, 200$ GeV at various centralities in full pseudorapidity range are well described, and the charged particle multiplicity are reproduced as functions of the number of participants. The energy dependence of the shape of the $dN_{ch}/d\eta$ distribution is also described at various collision energies $\sqrt{s_{NN}} = 200, 130, 62.4$ GeV in central collisions with same value of parameters except 19.6 GeV. The calculated rapidity distributions and yields for the charged pions and kaons in central Au+Au collisions at $\sqrt{s_{NN}} = 200$ GeV are compared with experimental data of the BRAHMS Collaboration.

PACS numbers: 13.87.Fh, 12.38.Bx, 12.40.-y

I. INTRODUCTION

The relativistic heavy ion collider (RHIC) at Brookhaven National Lab was built to search for quark matter, or the so-called quark-gluon plasma (QGP). Since its first run in 2000, a huge number of data have been accumulated and a comprehensive analysis of these data has been carried out. A variety of experimental facts from different aspects imply that the strongly coupled QGP has probably been produced in central Au+Au collisions at RHIC. For recent reviews of QGP and summary of experimental data, see e.g. [1, 2, 3, 4, 5, 6]. Central Au+Au collisions are characterized by the production of thousands of charged-particles in vacuum. The charged-particle density per unit rapidity or pseudorapidity dN_{ch}/dy or $dN_{ch}/d\eta$ is one of the most important observables to measure for the signal of QGP, from which a lot of information about the hot and dense matter can be extracted [7, 8, 9, 10, 11, 12, 13]. One can scale $dN_{ch}/d\eta$ or dN_{ch}/dy by the number of participant nucleon pairs $\langle N_{part}/2 \rangle$ and observe its logarithmic increase with $\langle N_{part} \rangle$, which is regarded as an evidence of color glass condensate [8, 9, 14, 15]. From the rapidity/pseudorapidity density and the transverse energy per particle, one can determine via Bjorken method the real density of the fireball which can provide one piece of evidence for the deconfinement phase transition. The experimental data about the charged-particle rapidity density have been presented by the PHOBOS collaboration [16, 17], the PHENIX collaboration [18], and the BRAHMS Collaboration [19, 20].

In this paper we will use a quark combination model to study the rapidity/pseudorapidity density varied with the number of participants and the energy in full rapidity range. The quark combination picture is successful in describing many features of multi-particle production in hadronic collisions. In ultra-relativistic heavy ion collisions at RHIC energies, a lot of new features are found, e.g. the high ratio of $n_p/n_\pi \sim 1$ at intermediate transverse momenta, which supports quark coalescence or recombination picture [21, 22, 23]. The quark number scaling of the elliptic flow is also a manifestation of the quark coalescence or recombination [24, 25, 26]. In this paper we will use a binary potential model for the constituent quark production and then let the constituent quarks combine into initial hadrons according to a quark combination rule. Then we allow the resonances in the initial hadrons to further decay to final hadrons with the help of the event generator PYTHIA 6.3 [27].

The paper is organized as follows. In the next section we give a brief description of the model for constituent quark production and combination. In section III, we present our predictions for the rapidity/pseudorapidity densities varied with the number of participants in the full rapidity range at $\sqrt{s_{NN}} = 130, 200$ GeV, the energy dependence of the $dN_{ch}/d\eta$ distribution at various collision energies for central collisions, and the results for the rapidity densities dN/dy and yields for charged pions and kaons in the central collisions at $\sqrt{s_{NN}} = 200$ GeV. The summary and discussions are in section IV.

II. THE QUARK PRODUCTION AND COMBINATION MODEL

In this section we give a brief introduction of the quark production and combination model we use. The model was first proposed for high energy e^+e^- and pp collisions [28, 29, 30, 31, 32, 33] and recently extended to ultra-relativistic heavy ion collisions [34, 35]. It has also been applied to the multi-parton systems in high energy e^+e^- annihilations [36, 37, 38, 39].

A. An effective model for quark production

The quark production from vacuum is a very sophisticated non-perturbative process. The color glass condensate model is a semi-classical QCD effective theory for the quark production in heavy ion collisions [14, 15]. In this paper we use a simple model for quark production which is of statistical nature without dynamic details. We determine the number of constituent quarks by the total effective energy for producing quarks from the vacuum excitation. The effective energy consists of the part for quark static masses and that for effective interquark potentials.

Consider a system of N_q quarks and anti-quarks excited in vacuum, the number of light and strange quarks/anti-quarks follow the ratio $N_u : N_d : N_s = 1 : 1 : \lambda_s$ with $N_q = N_u + N_d + N_s$, where $\lambda_s < 1$ is the strangeness suppression factor due to the heavier mass of strange quarks/anti-quarks. The average quark mass is given by $m = (2m_u + \lambda_s m_s)/(2 + \lambda_s)$, where $m_u = m_d$ is the light quark mass and m_s the strange quark mass.

We assume that the interaction is characterized by an inter-quark potential V which takes a substantial fraction of total effective energy. The constituent quark number can be determined from the following energy equation,

$$E = \langle N_q \rangle m + \frac{\langle N_q \rangle}{2} (\langle N_q \rangle - 1) \langle V \rangle, \quad (1)$$

which gives the number of constituent quarks as

$$\langle N_q \rangle = 2[(\alpha^2 + \beta E)^{1/2} - \alpha], \quad (2)$$

where

$$\beta \equiv \frac{1}{2\langle V \rangle}, \alpha \equiv \beta m - \frac{1}{4}. \quad (3)$$

Note that the quark number N_q follows a specific distribution, so does the potential, we have taken their averages in the above equations. In Eq. (1), we only included the two-body potential leading to a $E^{1/2} \sim s^{1/4}$ asymptotic behavior for N_q at high energy if $\langle V \rangle$ is constant. For a strong coupling system, it is possible that the n -body ($n > 2$) potential might be more important, and the asymptotic behavior then becomes $N_q \sim s^{1/2n}$. When n is large, N_q more and more approaches a logarithmic increase with energy.

The PHOBOS experiments have shown that above SPS energies, the total multiplicity per participant pair $\langle N_{\text{ch}} \rangle / \langle N_{\text{part}}/2 \rangle$ in central events scales with $\sqrt{s_{NN}}$ in the same way as e^+e^- collisions [17, 40]. This suggests a universal mechanism of particle production mainly controlled by the amount of effective energy available for particle production. Based on this property we extend the above quark production model originally applied to e^+e^- annihilation and pp collisions to heavy ion collisions. The average quark number in nucleus-nucleus collisions can be written as

$$\langle N_q \rangle = 2[(\alpha^2 + \beta \sqrt{s_{NN}})^{1/2} - \alpha] \langle N_{\text{part}}/2 \rangle, \quad (4)$$

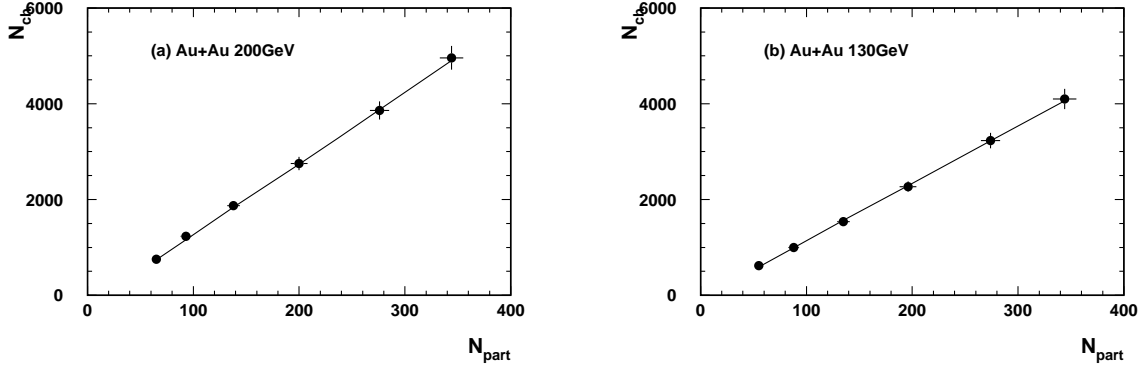
where we have taken $E = \sqrt{s_{NN}}$. Note that the effective energy E is equal to collision energy \sqrt{s} for light quark events in e^+e^- annihilation (but $E \neq \sqrt{s}$ for heavy quark events). Here we have assumed that the colliding nuclei is fully stopped and all the colliding energy $\sqrt{s_{NN}}$ is used for particle production, which is reasonable for the central collisions due to the fully rescatterings of partons towards the local equilibrium. It is also consistent with the Landau's space time evolution picture [41]. Note that the average number of quarks and antiquarks $\langle N_q \rangle$ includes not only new produced quarks and antiquarks, but also some additional quarks left by the incident nuclei.

B. Model for quark combination

In this subsection we briefly summarize how quarks combine into hadrons in our model. Different from many coalescence models which do not distinguish directly produced hadrons from final state hadrons, our quark combination model only describe the hadronization of initially produced hadrons including resonances. Then all resonances are allowed to decay into final state hadrons. Here we make use of the event generator PYTHIA 6.3 [27] to deal with resonance decays. The basic idea is to put N_q quarks and anti-quarks line up in a one-dimensional order in phase space, e.g. in rapidity, and let them combine into initial hadrons one by one following a combination rule. See section II of Ref. [34] for short description of such a rule. We note that it is very straightforward to define the combination in one dimensional phase space, but it is highly complicated to do it in two or three dimensional phase space [42]. The flavor SU(3) symmetry with strangeness suppression in the yields of initially produced hadrons is fulfilled in the model [28, 30]. Using the model, we have described most of multiplicity data for hadrons in electron-positron and

TABLE I: Yields of charged pions and kaons compared with BRAHMS data at 200 GeV [48].

	DATA	our model
π^+	$1660 \pm 15 \pm 133$	1676
π^-	$1683 \pm 16 \pm 135$	1680
K^+	$286 \pm 5 \pm 23$	280
K^-	$242 \pm 4 \pm 19$	242

FIG. 1: The centrality-dependent multiplicities of charged particles in Au+Au collisions at $\sqrt{s_{NN}} = 130, 200$ GeV. The solid lines are our results. The data are taken from PHOBOS [17].

proton-proton/anti-proton collisions [28, 29, 30, 31, 32, 33]. Also we solved a difficulty facing other quark combination models in describing the TASSO data for baryon-antibaryon correlation in electron-positron collisions [33]. Combined with the color flow picture [37], the model can describe the hadronization of multiparton states [36, 38, 39]. We have extended the model to reproduce the recent RHIC data for hadron multiplicity ratios, p_T spectra [34] and elliptic flows [35] in central rapidity region.

III. RAPIDITY AND PSEUDORAPIDITY DENSITIES

In this section, we use our combination model to compute the centrality dependence of distributions of rapidity/pseudorapidity densities in Au+Au collisions at $\sqrt{s_{NN}} = 130, 200$ GeV and study the energy dependence of the shape of the $dN_{ch}/d\eta$ distribution at various collision energies $\sqrt{s_{NN}} = 19.6, 62.4, 130$ and 200 GeV for central collisions, and also calculate the rapidity densities dN/dy and yields for charged pions and kaons in the central collisions at $\sqrt{s_{NN}} = 200$ GeV.

First we have to fix the parameters of the model. There are two parameters m and $\langle V \rangle$ or α and β in Eq.(2). As we pointed out that these quarks and antiquarks are constituent ones, so we use constituent masses $m_u = m_d = 0.34$ GeV and $m_s = 0.5$ GeV giving the average mass $m = 0.36$ GeV. The strangeness suppression factor is chosen to be $\lambda_s = 0.55$ by fitting the data at RHIC energies [34]. The parameter β is set to 3.6 GeV^{-1} which described the e^+e^- data. The parameters controlling the total multiplicity are the number of quarks and that of anti-quarks. In electron-positron and proton-antiproton collisions, the number of quarks is equal to that of anti-quarks, i.e. there are no excess baryons in contrast to anti-baryons. For nucleus-nucleus collisions, however, there are some excess baryons deposited by the colliding nuclei. The total number of quarks and anti-quarks $\langle N_q \rangle$ is given by Eq.(4). The number of net quarks can be further determined by the ratio of anti-proton to proton [34]. At 130 and 200 GeV, we find that the net quark numbers are about 420 and 360, respectively.

With these parameters, we calculate the centrality-dependent multiplicities of charged particles at $\sqrt{s_{NN}} = 130, 200$ GeV. The results are shown in Fig. 1 and agree with data very well.

In order to compute the distribution of rapidity/pseudorapidity densities with both energy and centrality dependence, we have to know the rapidity distribution of quarks and antiquarks before hadronization.

In the initial state, colliding nuclei are highly Lorentz contracted along the beam direction. After the initial

compression phase, the evolution of highly excited, and possibly deconfined, strongly interacting quark matter can be described by the ideal relativistic hydrodynamics. Under the assumption of full stopping and isentropic expansion, the amount of entropy (dS) contained within the (fluid) rapidity element dy in the Landau hydrodynamic picture is given by [41, 43, 44, 45, 46],

$$\frac{dS}{dy} = -\pi R^2 l s_0 \beta c_s \exp(\beta \omega_f) \left[I_0(q) - \frac{\beta \omega_f}{q} I_1(q) \right], \quad (5)$$

where $2\beta \equiv (1 - c_s^2)/c_s^2$ and $q \equiv \sqrt{\omega_f^2 - c_s^2 y^2}$ with $c_s^2 = (\frac{\partial P}{\partial \epsilon})_{\text{isentropic}}$ the sound velocity square. ω_f is related to the initial and freeze-out temperature T_f and T_0 by $\omega_f \equiv \ln(T_f/T_0)$. R is the radius of the nuclei. $2l$ is the initial longitudinal length. s_0 is the initial entropy density. I_0 and I_1 are the Bessel functions. The quantity $\pi R^2 l s_0$ is fixed to normalize the experimental data at mid rapidity. For $|\omega_f| \gg c_s y$ the quantity dS/dy can be approximated by a Gaussian distribution,

$$\frac{dS}{dy} \sim \frac{\exp(-\frac{y^2}{2\sigma^2})}{\sqrt{2\pi\sigma^2}}, \quad (6)$$

where

$$\sigma^2 = \frac{2|\omega_f|}{1 - c_s^2} \approx \frac{2c_s^2}{1 - c_s^4} \ln\left(\frac{s_{NN}}{2m_p m_\pi}\right). \quad (7)$$

where m_p is proton mass, m_π is pion mass, taken $T_f \approx m_\pi$. There is only one parameter c_s^2 left to be determined by experiments. dS/dy is proportional to dN/dy [47]. Therefore, the rapidity distribution for quarks and anti-quark before hadronization can be written as

$$\frac{dN}{dy} \sim \exp(-\frac{y^2}{2\sigma^2}), \quad (8)$$

We take the sound velocity square $c_s^2 = 1/4$ for QGP before hadronization ($c_s^2 = 1/3$ for ideal gas). We have used the fact that all quarks and anti-quarks are within the rapidity range $y \in [-4.2, 4.2]$ at 130 GeV and 200 GeV at all centralities of collisions.

With this input, we give $dN_{ch}/d\eta$ as functions of η at all available centralities at $\sqrt{s_{NN}} = 130, 200$ GeV. The results are shown in Fig. 2 and Fig. 3. One can see a good agreement between our model predictions and data in central collisions. For peripheral collisions, there is a slight deviation from data. The tails at large pseudorapidities especially in peripheral collisions are associated with remnants of collision spectators from the incoming nuclei. Therefore our results are slightly lower than data. Now we study the energy dependence of the shape of the η distribution of charged particles at various energies of Au +Au collisions. We compute pseudorapidity densities in full pseudorapidity range in most central collisions at $\sqrt{s_{NN}} = 62.4$ GeV and compare with BRAHMS data [49]. Here, the quark rapidity range is also $y \in [-4.2, 4.2]$ and the sound velocity square is also $c_s^2 = 1/4$ same as in 130 and 200 GeV. By studying we find that the shape of η distribution is mainly determined by the energy and the sound velocity and the the quark rapidity region only influences the forward pseudorapidity. The quark rapidity range is possible dependent of collision energy but not sensitive to that. The calculation results show that there is same value of the sound velocity for QGP in different collision energies above. This indicates a certain kind of universality for the quark matter produced in heavy-ion collisions at the late stage of evolution (before hadronization) at collision energies from 62.4 to 200 GeV. We also study the results at 19.6 GeV. We find that the model predictions disagree with the data using the constant value of the sound velocity square $c_s^2 = 1/4$ no matter how the quark rapidity region is chosen. We have to set the sound velocity $c_s^2 = 1/7$ and quark rapidity range $y \in [-3.2, 3.2]$. The change in the sound velocity might reflect the different properties of the matter produced at 19.6 GeV and at 62.4 GeV or higher energies. The model predictions are shown in Fig. 4 at $\sqrt{s_{NN}} = 19.6, 62.4, 130, 200$ GeV. The agreement with data is also satisfactory, which means that our model captures the energy behavior in the available collision energies.

To separate the trivial kinematic broadening of the $dN_{ch}/d\eta$ distribution from the more interesting dynamics, we also study the scaled, shifted pseudorapidity distribution $dN_{ch}/d\eta' / \langle N_{part}/2 \rangle$, where $\eta' = \eta - y_{beam}$, for Au+Au collisions at different energies. The calculation results are shown in Fig. 5 at $\sqrt{s_{NN}} = 19.6, 130, 200$ GeV and two centrality bins 0-6% and 35-40%. In most central collisions our model can describe the limit fragmentation very well. But in peripheral collisions there is a disagreement close to beam rapidity. The reason is that in peripheral collisions the beam rapidity region is dominated by spectators and is not covered by our model.

In ultra-relativistic heavy ion collisions at RHIC energies, charged pions and kaons are copiously produced. The yields of these light mesons carry the information on the entropy and strangeness created in the reactions. Here,

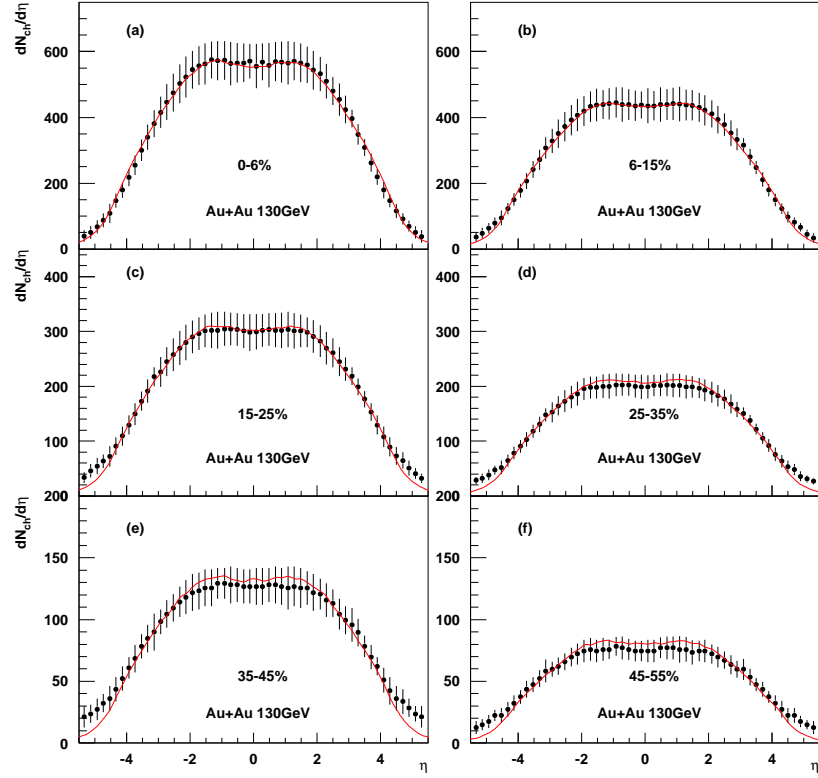


FIG. 2: Distributions of pseudorapidity density for charged particles in Au+Au collisions at $\sqrt{s_{NN}} = 130$ GeV for six centrality bins. The solid lines are our results. The data are taken from PHOBOS [17].

We calculate the rapidity density dN/dy and yields of charged pions and kaons in full rapidity for central Au+Au collisions (0 – 5%) at $\sqrt{s_{NN}} = 200$ GeV. The yields of charged pions and kaons compared with BRAHMS data [48] are shown in Tab. I. The results for rapidity density distributions of charged pions and kaons are shown in Fig. 6. Here, the pion yields are collected excluding the contributions of hyperon (Λ) and kaon K_{0s} decays. One can see that our model can well describe rapidity densities dN/dy and yields of charged pions and kaons in the whole rapidity range for central Au+Au collisions at $\sqrt{s_{NN}} = 200$ GeV.

IV. SUMMARY AND DISCUSSIONS

We study in a combination model the rapidity and pseudorapidity densities at various collision energies and centralities. We use the Landau relativistic hydrodynamic model to describe the evolution of highly excited and possibly deconfined quark matter. As a result, we obtain the Gaussian-type rapidity spectra of constituent quarks before hadronization. Then we use our combination model to describe the hadronization of initially produced hadrons including resonances, whose decays are dealt with by the event generator PYTHIA 6.3 [27]. We compute charged multiplicities and pseudorapidity densities at a variety of centralities at 130 and 200 GeV. The results for pseudorapidity densities are in good agreement with data in central collisions. In peripheral collisions, our predictions are slightly lower than data due to the fact that our model does not include the influence of the spectators. Our model can well describe the dependence of pseudorapidity densities and charged multiplicities on centralities and the number of participants respectively. We also calculate pseudorapidity densities at 19.6 and 62.4 GeV which describes the RHIC data very well. This means that our model can reproduce the collision energy dependence of pseudorapidity densities. However, We find that the value of the sound velocity square $c_s^2 = 1/7$ at 19.6 GeV is different from that at 62.4

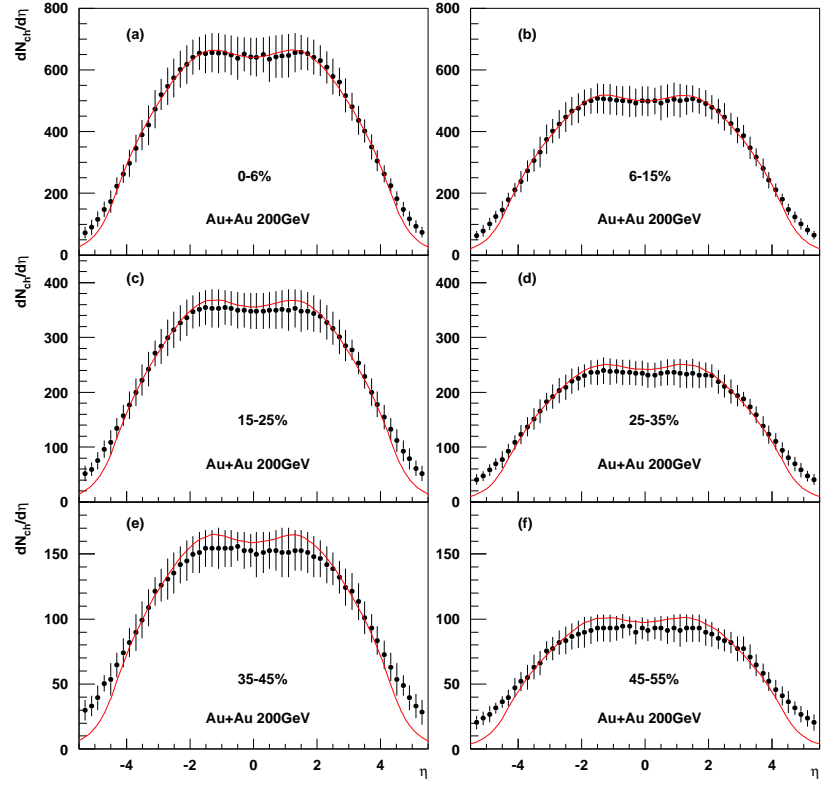


FIG. 3: Same as Fig. 2 but at $\sqrt{s_{NN}} = 200$ GeV.

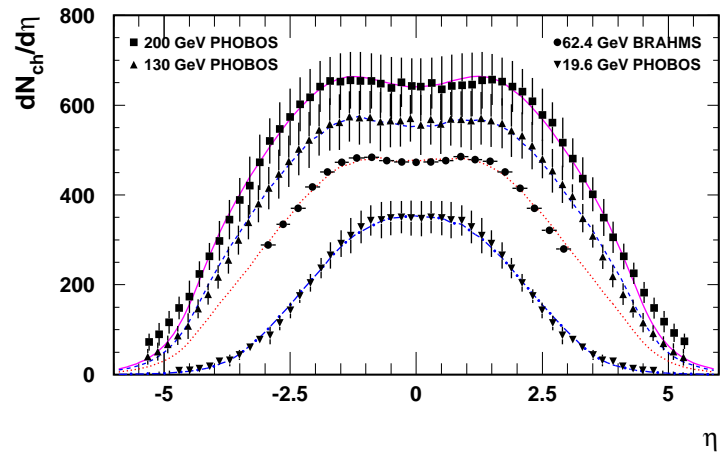


FIG. 4: Pseudorapidity densities $dN/d\eta$ for charged particles in most central collisions at various collision energies $\sqrt{s_{NN}} = 19.6, 62.4, 130, 200$ GeV. The lines are our results. The PHOBOS data are from Ref. [17], while the BRAHMS data are from Ref. [49].

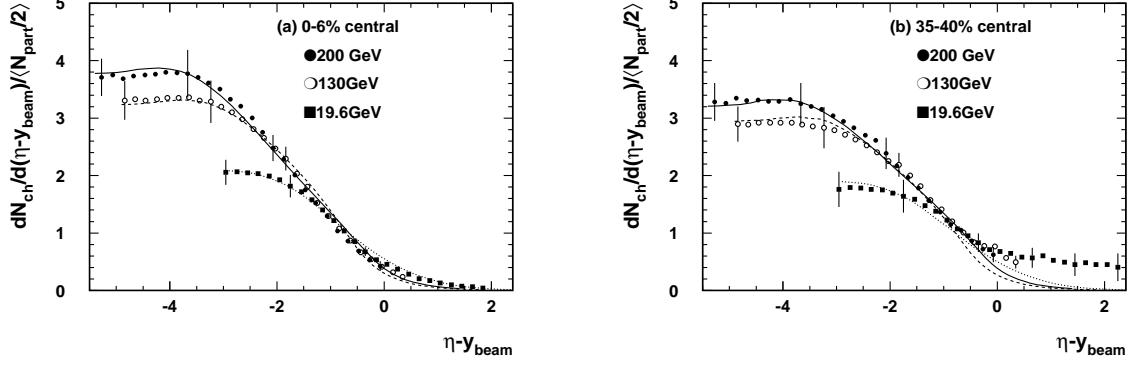


FIG. 5: The scaled, shifted pseudorapidity rapidity density at $\sqrt{s_{NN}} = 19.6, 130$ and 200 GeV. The results at two centrality bins are presented: $0\text{-}6\%$ and $35\text{-}40\%$. The lines are our results. The data are from Ref. [17],

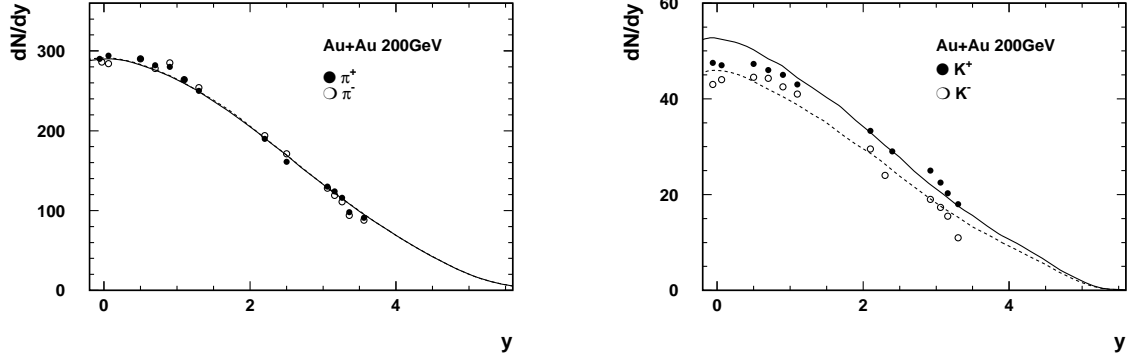


FIG. 6: dN/dy in the $0 - 5\%$ most central collisions at $\sqrt{s_{NN}} = 200$ GeV. The solid lines are π^+ and K^+ , and dashed lines are π^- and K^- . The data are given by BRAHMS collaborations [48].

GeV or higher energies. This imply that there is large change in properties of the hot and dense matter produced at collision energy between 19.6 and 62.4 GeV. To separate the trivial kinematic broadening of the distributions of the pseudorapidity density from more interesting dynamics, we compute the scaled and shifted pseudorapidity density distributions $dN_{ch}/d\eta'/(N_{part}/2)$ with $\eta' = \eta - y_{beam}$ at collision energies 19.6, 130 and 200 GeV. The good agreement with data is found except in the beam rapidity range of peripheral collisions, where our predictions are lower than data. Finally we present our results for rapidity densities of charged pions and kaons in most central collisions at 200 GeV. No contradiction to data is found. Note that the BRAHMS pion data do not include the decay products of K_s^0 and Λ , we also make the same corrections.

Acknowledgments

The authors thank Q. Wang, S.-Y. Li, and Z.-T. Liang for helpful discussions. The work is supported in part by the National Natural Science Foundation of China under the grant 10475049, the foundation of University Doctorate Educational Base of Ministry of Education under the grant 20030422064, and the science fund of Qufu Normal

University.

[1] J. Adams *et al.* [STAR Collaboration], Nucl. Phys. A **757**, 102 (2005) [arXiv:nucl-ex/0501009].

[2] M. Gyulassy and L. McLerran, Nucl. Phys. A **750**, 30 (2005) [arXiv:nucl-th/0405013].

[3] P. Jacobs and X. N. Wang, Prog. Part. Nucl. Phys. **54**, 443 (2005) [arXiv:hep-ph/0405125].

[4] P. F. Kolb and U. W. Heinz, arXiv:nucl-th/0305084.

[5] P. Braun-Munzinger, K. Redlich and J. Stachel, arXiv:nucl-th/0304013.

[6] D. H. Rischke, Prog. Part. Nucl. Phys. **52**, 197 (2004) [arXiv:nucl-th/0305030].

[7] X. N. Wang and M. Gyulassy, Phys. Rev. Lett. **86**, 3496 (2001) [arXiv:nucl-th/0008014].

[8] D. Kharzeev and M. Nardi, Phys. Lett. B **507**, 121 (2001) [arXiv:nucl-th/0012025].

[9] D. Kharzeev and E. Levin, Phys. Lett. B **523**, 79 (2001) [arXiv:nucl-th/0108006].

[10] A. Capella and D. Sousa, Phys. Lett. B **511**, 185 (2001) [arXiv:nucl-th/0101023].

[11] J. Dias de Deus and R. Ugoccioni, Phys. Lett. B **494**, 53 (2000) [arXiv:hep-ph/0009288].

[12] K. J. Eskola, K. Kajantie, P. V. Ruuskanen and K. Tuominen, Nucl. Phys. B **570**, 379 (2000) [arXiv:hep-ph/9909456].

[13] K. J. Eskola, K. Kajantie, P. V. Ruuskanen and K. Tuominen, Phys. Lett. B **543**, 208 (2002) [arXiv:hep-ph/0204034].

[14] L. D. McLerran and R. Venugopalan, Phys. Rev. D **49**, 2233 (1994) [arXiv:hep-ph/9309289].

[15] R. Venugopalan, Eur. Phys. J. C **43**, 337 (2005) [arXiv:hep-ph/0502190].

[16] B. B. Back *et al.* [PHOBOS Collaboration], Phys. Rev. Lett. **85**, 3100 (2000) [arXiv:hep-ex/0007036].

[17] B. B. Back *et al.*, [PHOBOS Collaboration], Phys. Rev. Lett. **91**, 052303 (2003) [arXiv:nucl-ex/0210015]; Phys. Rev. Lett. **87**, 102303 (2001) [arXiv:nucl-ex/0106006]; [arXiv:nucl-ex/0208003].

[18] K. Adcox *et al.* [PHENIX Collaboration], Phys. Rev. Lett. **86**, 3500 (2001) [arXiv:nucl-ex/0012008].

[19] I. G. Bearden *et al.* [BRAHMS Collaborations], Phys. Lett. B **523**, 227 (2001) [arXiv:nucl-ex/0108016].

[20] I. G. Bearden *et al.* [BRAHMS Collaboration], Phys. Rev. Lett. **88**, 202301 (2002) [arXiv:nucl-ex/0112001].

[21] R. J. Fries, B. Muller, C. Nonaka and S. A. Bass, Phys. Rev. Lett. **90**, 202303 (2003) [arXiv:nucl-th/0301087].

[22] V. Greco, C. M. Ko and P. Levai, Phys. Rev. Lett. **90**, 202302 (2003) [arXiv:nucl-th/0301093].

[23] R. C. Hwa and C. B. Yang, Phys. Rev. C **67**, 034902 (2003) [arXiv:nucl-th/0211010].

[24] S. A. Voloshin, Nucl. Phys. A **715**, 379 (2003) [arXiv:nucl-ex/0210014].

[25] D. Molnar and S. A. Voloshin, Phys. Rev. Lett. **91**, 092301 (2003) [arXiv:nucl-th/0302014].

[26] Z. w. Lin and C. M. Ko, Phys. Rev. Lett. **89**, 202302 (2002) [arXiv:nucl-th/0207014].

[27] T. Sjostrand, L. Lonnblad, S. Mrenna, and P. Skands, arXiv:hep-ph/0308153.

[28] Q. B. Xie and X. M. Liu, Phys. Rev. D **38**, 2169 (1988).

[29] Z. T. Liang and Q. B. Xie, Phys. Rev. D **43**, 751 (1991).

[30] Q. Wang and Q. B. Xie, J. Phys. G **21**, 897 (1995).

[31] J. Q. Zhao, Q. Wang and Q. B. Xie, Sci. Sin. A **38**, 1474 (1995).

[32] Q. Wang, Z. G. Si and Q. B. Xie, Int. J. Mod. Phys. A **11**, 5203 (1996).

[33] Z. G. Si, Q. B. Xie and Q. Wang, Commun. Theor. Phys. **28**, 85 (1997).

[34] F. I. Shao, Q. b. Xie and Q. Wang, Phys. Rev. C **71**, 044903 (2005) [arXiv:nucl-th/0409018].

[35] T. Yao, Q. b. Xie and F. I. Shao, arXiv:nucl-th/0606033.

[36] Q. Wang and Q. B. Xie, Phys. Rev. D **52**, 1469 (1995).

[37] Q. Wang, Q. B. Xie and Z. G. Si, Phys. Lett. B **388**, 346 (1996).

[38] Q. Wang, G. Gustafson and Q. b. Xie, Phys. Rev. D **62**, 054004 (2000) [arXiv:hep-ph/9912310].

[39] Q. Wang, G. Gustafson, Y. Jin and Q. b. Xie, Phys. Rev. D **64**, 012006 (2001) [arXiv:hep-ph/0011362].

[40] B. B. Back *et al.* [PHOBOS Collaboration], arXiv:nucl-ex/0301017.

[41] L. D. Landau, Izv. Akad. Nauk Ser. Fiz. **17**, 51 (1953).

[42] M. Hofmann, M. Bleicher, S. Scherer, L. Neise, H. Stocker and W. Greiner, Phys. Lett. B **478**, 161 (2000).

[43] S. Z. Belenkij and L. D. Landau, Nuovo Cim. Suppl. **3S10**, 15 (1956) [Usp. Fiz. Nauk **56**, 309 (1955)].

[44] B. Mohanty and J. e. Alam, Phys. Rev. C **68**, 064903 (2003) [arXiv:nucl-th/0301086].

[45] D. K. Srivastava, J. Alam, S. Chakrabarty, S. Raha and B. Sinha, Phys. Lett. B **278**, 225 (1992).

[46] D. K. Srivastava, J. e. Alam, S. Chakrabarty, B. Sinha and S. Raha, Annals Phys. **228**, 104 (1993).

[47] B. Mohanty, J. e. Alam and T. K. Nayak, Phys. Rev. C **67**, 024904 (2003) [arXiv:nucl-th/0208009].

[48] I. G. Bearden *et al.* [BRAHMS Collaboration], Phys. Rev. Lett. **94**, 162301 (2005) [arXiv:nucl-ex/0403050].

[49] P. Stasel (for BRAHMS Collaboration), Journal-ref: Nucl. Phys. A774 (2006) 77-92 [arXiv:nucl-ex/0510061].